nodes through lymphatic vessels is an important indicator of poor prognosis in many types of malignant tumors. Recently, much attention has been paid to the concept of 'sentinel lymph node' to which the tumor cells are first to lymphogeneously metastasize, e.g. it is reported that the pre- or intra-operative examination of sentinel lymph nodes is crucial for individualizing operative procedures to avoid extensive surgical resection [1].

The growing evidence for tumor-associated lymphangiogenesis, i.e. the formation of new lymphatic vessels in tumor tissues, has been accumulated in recent years [2,3]. Particularly, the correlation between lymphangiogenesis and lymph node metastases, i.e. whether the newly formed lymphatic vessels in tumor tissues facilitate metastasis to the lymph nodes, has been extensively investigated [4–11]. However, these studies were carried out largely by focusing on vascular endothelial growth factors (VEGFs) and their related molecules expressed in tumor tissues, and the morphological evidence indicating the presence of proliferating lymphatic vessels in carcinoma tissues remained to be unknown except the head and neck carcinoma [6,11].

The number of patients suffering from colorectal carcinoma has increased gradually in Japan, potentially due to changes in dietary habits [12]. However, morphological evidence that the lymphatic vessels actively proliferate in colorectal carcinoma has not been reported. The present study was undertaken to assay for proliferating lymphatic vessels in colorectal carcinoma tissues using a newly devised triple immunostaining method. Using this method, we statistically evaluated whether the degree of lymphangiogenesis in carcinoma tissues correlates with patients' prognosis as well as with various clinicopathological variables including lymph node metastasis.

2. Materials and methods

2.1. Patients' samples

Sixty-four patients, whose prognoses had been followed up at least for 5 years after surgical resection of colorectal carcinoma at the Department of Surgery, Shinshu University Hospital, Japan, were randomly chosen for the present study. Formalin-fixed and paraffin-embedded tissue blocks containing samples from these patients were retrieved from the archive of the Department of Laboratory Medicine, Shinshu University Hospital. Blocks represented carcinoma tissue and tissue with normal looking appearance removed away from carcinoma, and the latter is referred to as normal tissue. The average age of the patients was 65.6 (range 31–85) years old. Thirty-six patients (56.3%) were male, and 28 (43.7%) were female. Thirty-one patients (48.4%) presented with lymph node metastasis at the time of postoperative diagnosis. Forty-four patients (68.8%) had tumors with well differentiated adenocarcinoma, 16 (25.0%) with moderately differentiated adenocarcinoma, and 4 (6.3%) with poorly differentiated adenocarcinoma. The Ethical Committee of Shinshu University School of Medicine approved the study plans.

2.2. Immunohistochemistry

The triple immunostaining method described here utilized the following primary antibodies: anti-podoplanin antibody (AngioBio, Del Mar, CA, USA) to detect lymphatic endothelial cells [13], Ki-67 antibody (DakoCytomation, Glostrup, Denmark) to detect proliferating cells [14], and anti-human cytokeratin cocktail CK22 antibody (Biomeda, Foster City, CA, USA) to detect epithelial cells [15].

Briefly, 3 μm thick tissue sections were deparaffinized and dehydrated, and endogenous peroxidase activity was blocked by soaking in absolute methanol containing 0.3% H_2O_2 for 30 min. Before immunostaining, antigen retrieval was carried out by incubating tissue sections in a microwave in 10 mM Tris–HCl buffer (pH 8.0) containing 1 mM EDTA. Sections were blocked with 1% normal goat serum in 50 mM Tris buffered saline, pH7.6 (TBS) and incubated with the Ki-67 antibody for 60 min. After washing in TBS, slides were incubated with a secondary antibody, EnVision+ (DakoCytomation) for 45 min. 3,3-Diamino benzidine (DAB) was used as a chromogen. For the second round of immunostaining, the remaining peroxidase activity derived from EnVision+ was blocked by soaking in absolute methanol containing 0.3% H_2O_2 for 30 min. Sections were then incubated with the CK22 antibody for 60 min. After washing in TBS, slides were incubated with the EnVision+ (DakoCytomation) for 45 min, and the Vector VIP substrate kit for peroxidase (Vector, Burlingame, CA, USA) was used as a chromogen. For the third round of immunostaining, sections were incubated with anti-podoplanin antibody for 60 min. After washing in TBS, slides were incubated with the secondary antibody, alkaline phosphatase-conjugated rabbit anti-mouse immunoglobulins (DakoCytomation) for 45 min, and Vector blue alkaline phosphatase substrate kit III (Vector) was used as a chromogen. These slides were mounted with Dako Glycergel (DakoCytomation) mounting medium.

2.3. Evaluation of immunostaining

Evaluation of triple immunostaining was performed without knowledge of the clinical data. Lymphatic vessels were identified by both immunochemistry and the presence of tube-like structures. Under a microscope, three optical fields with the highest lymphatic vessel density (so-called 'hot spots' [16]) were identified in each sample at ×100 magnification. Lymphatic vessels were counted using ×200 magnification, corresponding to an optical field of 0.7386 mm^2. The lymphatic vessel density index (LDI),

Fig. 1. Lymphatic vessels in normal and carcinoma tissues of the colorectum. Anti-podoplanin immunoreactivity is seen as blue, Ki-67 as brown, and CK22 as violet. (A) Lymphatic vessels in normal colorectal tissues are mostly labeled by anti-podoplanin antibody alone. Note that a small artery (a) and vein (v) lack podoplanin immunoreactivity. (B) Lymphatic vessels in carcinoma tissue are doubly labeled by anti-podoplanin antibody and Ki-67 antibody but not by CK22 antibody (arrow). Bar = 100 μm.

which was defined as the sum of lymphatic vessels measured in three hot spots, was calculated.

Proliferating lymphatic vessels, which were positive for podoplanin and Ki-67 antigen but negative for cytokeratin, were counted in the same three hot spots as described above, and then the ratio of proliferating lymphatic vessels to all lymphatic vessels in the optical fields was defined as the proliferation index (PI).

2.4. Statistical analysis

Statistical analyses were performed using SPSS software version 12.0 (SPSS/ Inc., Chicago, IL, USA). Comparisons of LDI and PI in carcinoma tissue versus normal tissue were carried out by the Mann–Whitney U-test. Analyses of 5-year survival of patients based on the degree of LDI or PI were carried out using the Kaplan–Meier method. Statistical analyses correlating LDI or PI and various clinicopathological variables were carried out by χ^2-test. Differences were considered significant when the P-values of <0.05 were obtained.

3. Results

3.1. Detection of proliferating lymphatic vessels

Lymphatic vessels were identified by positive immunoreactivity for podoplanin. In the normal colorectal tissues, lymphatic vessels were frequently found adjacent to the muscularis mucosae as thin-walled and tube-like structures exhibiting a distinct inner cavity (Fig. 1A). By contrast, lymphatic vessels in carcinoma tissues were observed mostly in the peritumoral area and occasionally seen in the intratumoral area (Fig. 1B). Vessels in carcinoma tissues showed various morphological features such as flattening, thickened walls, and smaller size relative to those observed in normal mucosa.

Proliferating lymphatic vessels were identified as doubly labeled with anti-podoplanin and Ki-67 antibodies and negative for the CK22 cytokeratin antibody. Significantly, such proliferating cells were seen with greater frequency in carcinoma tissues than in normal tissues (Fig. 1). Triple immunostaining allowed us to easily exclude Ki-67-positive carcinoma cells found on the margin of lymphatic vessels from proliferating lymphatic cells by their positive immunoreactivity to CK22 antibody (Fig. 2).

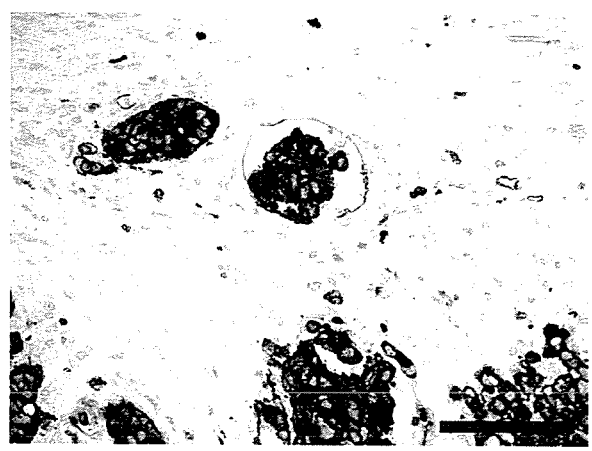

Fig. 2. Proliferating colorectal carcinoma cells in lymphatic vessels. Adenocarcinoma cells that proliferate in lymphatic lumens are identified by positive immunoreactivity to CK22 antibody (violet) and Ki-67 (brown) antibody but not anti-podoplanin antibody (blue). Bar = 100 μm.

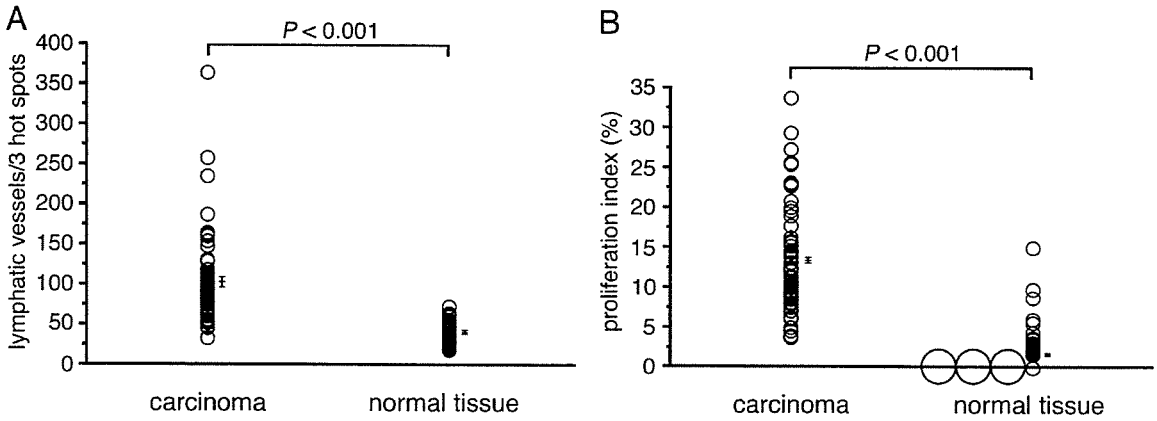

Fig. 3. Scatter diagrams of lymphatic vessel density index (LDI) and proliferation index (PI) in carcinoma and normal tissues. Both LDI (A) and PI (B) in carcinoma tissues are significantly higher than those in normal tissues. Small and large circles represent 1 and 10 patients, respectively. Vertical bars indicate means ± standard errors.

3.2. Evidence of lymphangiogenesis in colorectal carcinoma

In order to test whether lymphangiogenesis was occurring in colorectal carcinoma tissues, both the number of lymphatic vessels observed in three 'hot spot' areas of carcinoma tissues and the ratio of proliferating lymphatic vessels to all lymphatic vessels found in the same areas were assessed by measuring lymphatic vessel density index (LDI) and proliferation index (PI), respectively. Then, these indexes were compared with those of normal tissues.

As shown in Fig. 3A, LDI of carcinoma tissues was determined to be 102.7 ± 6.7 (mean ± standard error) vessels/3 hot spots, whereas LDI of normal tissues was found to be 39.9 ± 1.5 vessels/3 hot spots. Statistical analysis revealed that LDI of carcinoma tissues was significantly higher than that of normal tissues ($P < 0.001$). PI of carcinoma tissues was determined to be 13.3 ± 0.8%, while PI of normal tissues was 1.6 ± 0.3% (Fig. 3B). Again, PI of carcinoma tissues was significantly higher in comparison with PI of normal tissue ($P < 0.001$). Taken together, these results indicate that lymphangiogenesis occurs in colorectal carcinoma.

3.3. Clinicopathological significance of lymphangiogenesis in colorectal carcinoma

Finally, we examined the clinicopathological significance of lymphangiogenesis occurring in colorectal carcinoma. LDI measured in carcinoma tissues was used to place patients into two categories: those above the median values of LDI (89.0 vessels/3 hot spots) defined as the high LDI group, and those lower than the median value defined as the low LDI group. Similarly, PI evaluated in carcinoma tissues was also used to classify patients into two categories: those above the median values of PI (11.5%) defined as the high PI group, and those lower than the median value defined as the low PI group.

Unexpectedly, 5-year survival analysis of all the 64 patients determined by the Kaplan–Meier method revealed that the patients' outcome was not significantly different between the high LDI group and the low LDI group ($P = 0.864$), and similar results were also found between the high PI group and the low PI group ($P = 0.854$). Because distant metastasis, which might affect the patients' prognoses, was present at the time of operation in Duke's D patients, we have then analyzed 45 patients, excluding Duke's D. However again, no significant differences were obtained for LDI ($P = 0.346$) and PI ($P = 0.617$). We next compared the high LDI group and the low LDI group in respect to various clinicopathological variables such as lymph node metastasis and clinical stage determined by Duke's classification, but no significant difference was observed between these two groups (Table 1). The same analyses were also performed between the high PI group and the low PI group, but no significant difference was obtained.

4. Discussion

In the present study, we have demonstrated that lymphangiogenesis occurs in colorectal carcinoma. To do so we devised a triple immunostaining method evaluating immunoreactivity for Ki-67 antigen as a marker of proliferation, for cytokeratin as an epithelial cell marker, and for podoplanin as a

Table 1
Association of lymphatic density and PI with clinicopathological parameters

	Subject ($n=64$)	LDI		P	PI		P
		Low (%)	High (%)		Low (%)	High (%)	
Location[a]							
Proximal	28	12(42.9)	16(57.1)	0.313	12(42.9)	16(57.1)	0.431
Distal	36	20(55.6)	16(44.4)		19(52.8)	17(47.2)	
Histopathology[b]							
Well	44	24(54.5)	20(45.5)	0.281	23(52.3)	21(47.7)	0.362
Moderate+poor	20	8(40.0)	12(60.0)		8(40.0)	12(60.0)	
Lymph node metastasis							
Negative	33	18(54.5)	15(45.5)	0.453	15(45.5)	18(54.5)	0.622
Positive	31	14(45.2)	17(54.8)		16(51.6)	15(48.4)	
Duke's classification[c]							
A	6	3(50.0)	3(50.0)	0.956	4(66.7)	2(33.3)	0.558
B	21	11(52.4)	10(47.6)		8(38.1)	13(61.9)	
C	18	8(44.4)	10(55.6)		10(55.6)	8(44.4)	
D	19	10(52.6)	9(47.4)		9(47.4)	10(52.6)	
Lymphatic vessel invasion							
Negative	7	3(42.9)	4(57.1)	0.689	5(71.4)	2(28.6)	0.197
Positive	57	29(50.9)	28(49.1)		26(47.4)	31(52.6)	

[a] 'Proximal' indicates cecum, ascending colon, and transverse colon, while 'distal' indicates descending colon, sigmoid colon, and rectum.
[b] 'Well' indicates well differentiated adenocarcinoma, while 'moderate' and 'poor' indicate moderately and poorly differentiated adenocarcinoma, respectively.
[c] A, confined to the intestinal wall; B, complete penetration of the intestinal wall; C, presence of nodal involvement; D, presence of distance metastasis.

lymphatic vessel-specific marker. This method identifies proliferating lymphatic vessels as podoplanin and Ki-67 positive and distinguishes proliferating carcinoma cells in the lymphatic lumen from proliferating lymphatic endothelial cells by the positive immunoreactivity to cytokeratin seen in the former. This method is advantageous over double immunostaining methods used in our preliminary studies in which the anti-podoplanin antibody and Ki-67 antibody positivity could not determine whether Ki-67-positive cells at the margin of lymphatic vessels were lymphatic endothelial cells or carcinoma cells that had invaded lymphatic vessels (data not shown).

Recently, growing evidence has accumulated that lymphangiogenesis occurs and plays a role in carcinoma: specifically, the expression level of vascular endothelial growth factors (VEGFs) and/or their receptors in carcinoma cells has been positively associated with lymph node metastasis and poor prognosis [4,5,7–9]. In particular, in colorectal carcinoma, it has been reported that the expression level of VEGF-D cytokine and the VEGF receptor VEGFR-3 in the carcinoma tissues are significantly higher than those in the normal tissues [7]. The same study also demonstrated that transcriptional levels of the lymphatic endothelial markers, Prox-1, 5′-nucleotidase, and podoplanin, were significantly higher in colorectal carcinoma tissues than those in normal tissues, suggesting that lymphangiogenesis occurs in colorectal carcinoma. However, there has been no morphological evidence for lymphangiogenesis in colorectal carcinoma such as the demonstration of proliferating lymphatic endothelial cells. Here, we provide such evidence by showing that both LDI and PI, which are indicators of lymphatic vessel density and growth fraction of lymphatic vessels, were dramatically elevated in colorectal carcinoma tissues compared to normal tissues (see Fig. 3). Future study will be necessary to investigate the correlation between the lymphatic vessel proliferation (LDI and PI) and expression of lymphagiogenic factors such as VEGFs in this series of patients examined in the present study.

In the present study, we did not observe significant positive correlations between the degree of lymphangiogenesis and clinical outcome. However, this result does not simply exclude the possibility that lymphangiogenesis plays a role in the prognosis of colorectal carcinoma, because the limited number of the patients was examined in this study. Relevant to the present results, Wong et al., recently demonstrated that the expression level of VEGF-C secreted by a subline of prostate cancer PC-3 cells transplanted in nude mice is

positively correlated with increased lymphatic vessel density, but the lymph node metaistasis was not associated with the lymphangiogenesis thus formed [10]. By contrast, Kyzas et al. demonstrated that lymphangiogenesis found in head and neck squamous cell carcinoma is closely associated with patients' survival [11]. These results as a whole indicate that the clinicopathological significance whether lymphangiogeneis affects the patients' survival rate or not might depend on the tumor type as well. It will be of great significance to determine the correlation between lymphoangiogenesis and prognosis of the patients in various types of cancer by using the triple immunostaining method developed in the present study.

Acknowledgements

We thank Drs Fukuto Maruta and Atsushi Sugiyama for encouragement during this study, Ms Akiko Ishida for technical assistance, and Dr Elise Lamar for critical reading of the manuscript. This work was supported by a Grant-in-Aid for Scientific Research B-15390115 from the Japan Society for the Promotion of Science (to J.N.).

References

[1] Y. Kitagawa, M. Kitajima, Gastrointestinal cancer and sentinel node navigation surgery, J. Surg. Oncol. 79 (2002) 188–193.
[2] M.S. Pepper, J.C. Tille, R. Nisato, M. Skobe, Lymphangiogenesis and tumor metastasis, Cell Tissue Res. 314 (2003) 167–177.
[3] T. Ohhashi, R. Mizuno, F. Ikomi, Y. Kawai, Current topics of physiology and pharmacology in the lymphatic system, Pharmacol. Ther. 105 (2005) 165–188.
[4] S.A. Stacker, C. Caesar, M.E. Baldwin, G.E. Thornton, R.A. Williams, R. Pervo, et al., VEGF-D promotes the metastatic spread of tumor cells via the lymphatics, Nat. Med. 7 (2001) 186–191.
[5] M. Skobe, T. Hawighorst, D.G. Jackson, R. Prevo, L. Janes, P. Velasco, et al., Induction of tumor lymphangiogenesis by VEGF-C promotes breast cancer metastasis, Nat. Med. 7 (2001) 192–198.
[6] N.J. Beasley, R. Prevo, S. Banerji, R.D. Leek, J. Moore, P. van Trappen, et al., Intratumoral lymphangiogenesis and lymph node metastasis in head and neck cancer, Cancer Res. 62 (2002) 1315–1320.
[7] C. Parr, W.G. Jiang, Quantitative analysis of lymphangiogenic markers in human colorectal cancer, Int. J. Oncol. 23 (2003) 533–539.
[8] R. Cao, M.A. Bjorndahl, P. Religa, S. Clasper, S. Garvin, D. Galter, et al., PDGF-BB induces intratumoral lymphangiogenesis and promotes lymphatic metastasis, Cancer Cell 6 (2004) 333–345.
[9] K. Shimizu, H. Kubo, K. Yamaguchi, K. Kawashima, Y. Ueda, K. Matsuo, et al., Suppression of VEGFR-3 signaling inhibits lymph node metastasis in gastric cancer, Cancer Sci. 95 (2004) 328–333.
[10] S.Y. Wong, H. Haack, D. Crowley, M. Barry, R.T. Bronson, R.O. Hynes, Tumor-secreted vascular endothelial growth factor-C is necessary for prostate cancer lymphangiogenesis, but lymphangiogenesis is unnecessary for lymph node metastasis, Cancer Res. 65 (2005) 9789–9798.
[11] P.A. Kyzas, S. Geleff, A. Batistatou, N.J. Agnantis, D. Stefanou, Evidence of lymphangiogenesis and its prognostic implications in head and neck squamous cell carcinoma, J. Pathol. 206 (2005) 170–177.
[12] S. Kono, Secular trend of colon cancer incidence and mortality in relation to fat and meat intake in Japan, Eur. J. Cancer Prev. 13 (2004) 127–132.
[13] S. Breiteneder-Geleff, A. Soleiman, H. Kowalski, R. Horvat, G. Amann, E. Kriehuber, et al., Angiosarcomas express mixed endothelial phenotypes of blood and lymphatic capillaries: podoplanin as a specific marker for lymphatic endothelium, Am. J. Pathol. 154 (1999) 385–394.
[14] J. Gerdes, U. Schwab, H. Lemke, H. Stein, Production of a mouse monoclonal antibody reactive with a human nuclear antigen associated with cell proliferation, Int. J. Cancer 31 (1983) 13–20.
[15] M. Perez-Guillermo, J. Sola-Perez, C. Abad-Montano, F.A. Pastor Quirante, M.S. Montalban Romero, Merkel cell tumor of the eyelid and the cytologic aspect in fine-needle aspirates: report of a case, Diagn. Cytopathol. 10 (1994) 146–151.
[16] N. Weidner, J.P. Semple, W.R. Welch, J. Folkman, Tumor angiogenesis and metastasis—correlation in invasive breast carcinoma, N. Engl. J. Med. 324 (1991) 1–8.

J Hepatobiliary Pancreat Surg (2006) 13:105–109
DOI 10.1007/s00534-005-1015-y

Journal of HBP Surgery

Risk factors contributing to hepatic artery thrombosis following living-donor liver transplantation

Toshihiko Ikegami[1], Yasuhiko Hashikura[1], Yuichi Nakazawa[1], Koichi Urata[1], Atsuyoshi Mita[1], Yasunari Ohno[1], Masaru Terada[1], Shin-ichi Miyagawa[1], Hideo Kushima[2], and Shoji Kondoh[2]

[1]Department of Surgery, Shinshu University School of Medicine, 3-1-1 Asahi, Matsumoto 390-8621, Japan
[2]Department of Plastic Surgery, Shinshu University School of Medicine, Matsumoto, Japan

Abstract
Background/Purpose. This study was carried out to investigate the risk factors contributing to hepatic artery thrombosis in living-donor liver transplantation.
Methods. Two hundred and twenty-two recipients (113 adults and 109 children) of living-donor liver transplantation were the subjects of this study. The diagnosis of hepatic artery thrombosis was made by color-Doppler ultrasonography and/or hepatic angiography. Parameters for this study were: (1) donor sex, age, and body weight; (2) recipient sex, age, body weight, liver disease, preoperative prothrombin time, and type of arterial reconstruction; and (3) previous liver transplantation.
Results. Hepatic artery thrombosis occurred in 12 patients (5.4%) at 3 to 15 days posttransplant. Recipient female sex and metabolic disorder as the original disease were found to be significantly associated with hepatic artery thrombosis. The 5-year patient survival rate in recipients with hepatic artery thrombosis (58.3%) was significantly lower than that in recipients without this complication (84.4%).
Conclusions. Female sex and metabolic disease may be factors contributing to hepatic artery thrombosis after living-donor liver transplantation. More intensive anticoagulation therapy for this patient population might decrease the incidence of hepatic artery thrombosis and, thus, posttransplant recipient mortality.

Key words Sex · Metabolic liver disease · Vascular reconstruction · Anticoagulation

Introduction

Hepatic artery thrombosis (HAT) after orthotopic liver transplantation can lead to ischemia of the liver graft, which can result in graft morbidity or loss or even patient death, because the potential collateral supply to the graft is disrupted at the time of recipient hepatectomy and the transplanted liver is particularly dependent on hepatic arterial blood flow. Retransplantation used to be the only possible therapy for HAT in up to 75% of patients, with a mortality rate approaching 50%.[1] Although urgent revascularization may avoid the need for retransplantation,[2] early diagnosis is an essential prerequisite for this strategy.[3] Technological innovations in color Doppler ultrasonography have provided an accurate noninvasive method for the detection of hepatic artery thrombosis before irreversible ischemic damage of the allograft occurs.[4,5]

Early experience in living-donor liver transplantation (LDLT) was plagued by HAT. Rates of HAT were as high as 28%, and the high incidence of arterial thrombosis in early series led to adoption of the use of an operating microscope.[6] Many LDLT centers have now introduced the operating microscope.

The aim of the present study was to review, retrospectively, our experience with 222 LDLTs from June 1990 to December 2004 at a single institution, with the intention of performing univariate and multivariate analyses to identify factors associated with the development of HAT.

Patients and methods

From June 21 1990 through December 31 2004, 222 consecutive LDLTs were performed in 219 patients at our institution. All LDLTs were approved by the Shinshu University Ethics Committee. The recipients were 113 adults and 109 children. The analysis was performed with a mean follow-up of 1777 days (range, 30–5315). The patients were 24.6 ± 23.0 years old (mean ± SD; range, 0.3–69.4 years) at the time of the LDLT, and weighed 33.7 ± 22.5 kg (mean ± SD; range, 4.0–83.5 kg). The median age of the adults was 44.7 years (range, 18–69 years) and that of the children was 1.3 years (range,

Offprint requests to: Y. Hashikura
Received: April 30, 2005 / Accepted: May 30, 2005

4 months to 16 years). The primary disease leading to the need for LDLT was biliary atresia in 80 patients, viral hepatitis in 27, fulminant hepatic failure in 26, familial amyloid polyneuropathy in 25, primary biliary cirrhosis in 23, citrullinemia in 10, primary sclerosing cholangitis in 8, Alagille's syndrome in 5, and others in 18. The donors were the patients' parents for 129 patients, children for 42, spouses for 19, siblings for 22, grandparent for 1, nephew for 1, cousin for 1, and domino donors for 7. Sixty-six liver grafts were left-lateral segments, 26 were extended-lateral segments, 104 were left lobes, 21 were left lobes with caudate lobes, 4 were right lobes, and 1 was a posterior segment.

Donor operation

Preoperative evaluation for potential living-related liver donors included a complete history and physical examination, abdominal computed tomography (CT) scan, and angiography. The CT scan was used to calculate the size of the whole liver, left lobe, and left lateral segment.[7] Prior to 2003, angiography was used to assess the hepatic arterial supply, especially to the potential graft, and the diameters of the hepatic arteries. Thereafter, three-dimensional (3D) CT was used for this purpose.

The donor hepatectomy was performed by a technique described previously.[8] The type of liver graft used was dependent on the body build of the recipient and on the calculated segmental volume of the donor liver. The whole right lobe was harvested only in domino LDLT. A left-lobe graft with or without the caudate lobe was used in 108 of the 113 adult patients and was the most common type of liver graft used.

All grafts were preserved with University of Wisconsin solution.

Recipient operation

An end-to-end interrupted suture with 8-0, 9-0, or 10-0 nonabsorbable nylon monofilament sutures was used for arterial anastomosis, performed under the operating microscope, except for the first ten cases, in which a surgical loupe was used. Eight stitches were initially used for vessel anastomoses. In recipients in whom there was only one graft hepatic arterial input, this was anastomosed to the recipient artery. For 86 patients, the graft had multiple arterial inputs. In 65 of these patients, the thickest artery was reconstructed first and pulsatile blood backflow was observed from the arterial stumps that had not been anastomosed. In these patients, after we had confirmed intrahepatic arterial blood flow by intraoperative color-Doppler ultrasound, the remaining arteries were not anastomosed. In contrast, in 21 patients, pulsatile bleeding from the nonanastomosed stumps was not observed after rearterialization of the largest artery, and all graft arteries were anastomosed to the recipient arteries.[9]

The recipient left or right hepatic artery was used for reconstructions in most cases. In three patients, the right gastroepiploic or the jejunal artery was used because their hepatic arteries were damaged. A vascular interposition graft was used in two patients.

Color-Doppler ultrasound was performed immediately after hepatic arterial reconstruction and during the closure of the abdominal wall to demonstrate patency of the anastomosis.

Postoperative management

Initially, immunosuppression was performed with cyclosporine, azathioprine, and steroids, and this protocol was used until September 1993. Tacrolimus and steroids have been used since October 1993. As postoperative anti-coagulation therapy, low-dose low-molecular-weight heparin, antithrombin, protease inhibitor, and prostaglandin E_1 were administered intravenously. Fresh frozen plasma was also given to supply anticoagulants. The hematocrit of the patient was kept below 30% to minimize the blood viscosity.

Color-Doppler ultrasound was performed on each postoperative day in all recipients to confirm the patency of the intrahepatic arteries. We defined HAT as the complete occlusion of arterial blood flow to the allograft; the diagnosis was based on color-Doppler ultrasound findings and confirmed by means of 3D CT and/or hepatic angiography.

Analysis of risk factors

To explore the factors contributing to posttransplant HAT in LDLT, we analyzed the etiology of the recipient liver disease (metabolic vs nonmetabolic); previous liver transplantation; donor sex and age (equal to or more than 60 years old, or less); recipient sex; age (equal to or more than 18 years old, or less); body weight (equal to or more than 15 kg, or less); and preoperative prothrombin time, recipient/donor body weight ratio, and type of arterial anastomosis (reconstruction of all arterial inputs vs partial reconstruction of arterial inputs).

Statistical analysis

Univariate analysis was performed for categorical variables, with the use of the Mann-Whitney *U*-test to identify independent risk factors for HAT after LDLT. We analyzed continuous variables with a two-tailed unpaired *t*-test. On univariate analysis, $P = 0.005$ was considered significant. Variables with P values of less than

0.05 in the univariate analysis were entered into a forward stepwise logistic regression analysis to estimate the odds ratio (OR) of each artery complication (dependent variables) and the presence or absence of potential prognostic factors (independent variables). The OR was defined as exp(β-coefficient) with 95% confidence intervals (CIs). Kaplan-Meier estimates were used to calculate graft survival curves. Differences in survival curves were compared by log-rank statistics.

Results

All hepatic arterial anastomoses were patent immediately after reconstruction. HAT occurred in 12 patients, which corresponds to 5.4% of all recipients. The time interval between transplantation and the diagnosis of HAT ranged from 3 to 15 days (mean, 6.8 days; median, 6.5 days).

Previous liver transplantation, and donor sex age; recipient age, body weight, and preoperative prothrombin time; recipient/donor body weight; and type of arterial anastomosis were found not to be associated with the occurrence of HAT, whereas recipient sex and liver disease were found to be significantly associated with HAT. The incidence of HAT in the 136 female patients was significantly higher than that in male patients (8.1% vs 1.2%; $P = 0.027$). HAT was more common among the 39 recipients who needed liver transplantation for metabolic disease (12.8%) than in the 183 who needed transplantation for nonmetabolic disease (3.8%; $P = 0.024$; Table 1).

By logistic regression, recipient sex (OR, 4.023; 95% confidence interval [CI], 1.04–65.0; $P = 0.045$) and etiology of recipient liver disease (OR, 4.22; 95% CI, 1.07–12.00; $P = 0.040$) proved to be independent predictors of HAT. HAT developed in 5 of 26 recipients (19.2%) who had the simultaneous presence of these two factors (OR, 6.43; 95% CI, 1.87–22.1).

Of the 12 HAT patients, 11 were treated surgically. One patient, who was diagnosed as having HAT on the seventh postoperative day, with simultaneous thrombo-

Table 1. Risk factors associated with HAT

Variables/category	Incidence of hepatic artery thrombosis	*P*
Donor sex		0.6726
Male	7/122	
Female	5/100	
Donor age		0.5896
≧60 Years	0/5	
<60 Years	12/217	
Previous transplantation		0.6775
Yes	0/3	
No	12/219	
Recipient sex		0.0266
Male	1/86	
Female	11/136	
Metabolic disease		0.0244
Yes	5/39	
No	7/183	
Recipient age		0.2624
<18 Years	4/109	
≧18 Years	8/113	
Recipient body weight		0.8414
<15 kg	4/80	
≧15 kg	8/142	
Ratio of recipient's body weight to donor's body weight		0.2921
<1.25	11/215	
≧1.25	1/7	
Prothrombin time		0.2919
<13 s	5/63	
≧13 s	7/159	
Blood type		0.1644
Identical	7/167	
Nonidentical	5/55	
Hepatic arterial reconstruction		0.7515
All	8/157	
Partial	4/65	

sis of the portal vein, was treated without operation, and she died. Among the 11 surgically treated patients, 9 patients were successfully revascularized (removal of the thrombus and refashioning of the arterial anastomosis), but 3 of them died, as a result of aspergillosis, lung edema, and liver abscess, respectively. Revascularization failed in 2 patients, one of whom was retransplanted successfully, and the other died.

Overall actuarial patient and graft 5-year survival rates were 83.0% and 82.1% (Kaplan-Meier analysis). The patient survival rates for the HAT patients ($n = 12$) were 58.3%, 58.3%, and 58.3% at 1, 3, and 5 years, respectively. The graft survival rates were 50.0%, 50.0%, and 50.0% at 1, 3, and 5 years, respectively. These rates were significantly worse than those for patients who did not develop HAT ($P = 0.0015$ for patient survival and $P < 0.001$ for graft survival).

Discussion

HAT is still one of the main causes of graft loss after liver transplantation. Its incidence remains high, even in the more recent reports from highly specialized and experienced transplantation units, which makes it hard to ascribe to difficulties in handling what is now a well-established technique. In the series from the University of Pittsburgh, even in the more recent era of retrospective analysis of 4000 consecutive transplants, HAT was the indication for nearly one-third of the retransplantations performed.[10]

Various factors contributing to development of vascular thrombosis have been proposed: technical problems,[2,3,11] pediatric recipients, prolonged cold ischemic time,[12,13] severe hypotension,[2] the presence of a postoperative hematocrit of more than 44%,[14] cytomegalovirus (CMV) infection,[15,16] and acute rejection.[17]

In our present patients, there was neither hypotension nor rejection prior to HAT. The ischemic time was fairly short (106 ± 23 min), and technical problems were not observed at the time of reoperation. The hematocrit prior to HAT was kept below 44% in all patients with HAT. CMV infection and acute rejection were not diagnosed in our HAT patients.

Recently, Oh et al.[18] showed that a recipient body weight of less than 15 kg or a recipient/donor body weight ratio of greater than 1.25 were risk factors for ischemic graft complications. The results from our series do not support these observations.

Vivarelli et al.[19] reported that donor age greater than 60 years was a predictor of HAT. In our current study, donor age greater than 60 years was not a risk factor for HAT. In our series, candidate donors older than 60 years underwent rigorous examination to rule out the risk factors for donor hepatectomy, and candidates who had diabetes mellitus or uncontrolled hypertension were excluded. This procedure could decrease the number of donors with atherosclerosis and, consequently, also decrease the possibility of older donors representing a risk factor for HAT.

In our study, recipients with metabolic liver disease had a significantly higher risk of HAT than did those with nonmetabolic liver disease. The metabolic liver-disease group included 25 patients with familial amyloid polyneuropathy, 10 with citrullinemia, 1 with carbamylphosphate synthetase deficiency, 1 with Wilson's disease, and 1 with glycogen storage disease type 1a. Their liver functions, especially synthetic function, were almost normal, except for the single patient with Wilson's disease. In such patients (i.e., those without coagulopathy), not only is the coagulation state likely to be normal but also the platelet count is not decreased and the hematocrit may be high, unlike the situation in patients with cirrhosis or fulminant hepatic failure. This may be one of the reasons why this group experiences the complication of HAT more often. The incidence of HAT in patients with prothrombin time less than 13 s, showed a tendency to be higher than that in patients with prothrombin time longer than 13 s, although the difference did not reach statistical significance. Together, these data indicate that patients with metabolic disease require more intensive posttransplant anticoagulation therapy.

Another risk factor in our series was recipient sex. Female recipients experienced HAT more frequently than did male recipients. We are unable to explain this observation.

Our rate of HAT, 5.4%, is similar to that reported for cadaver liver transplants, of approximately 7% (range, 4% to 25%).[12,20,21]

Once the diagnosis of HAT after liver transplantation has been confirmed, retransplantation has been considered the standard treatment in the majority of cases, although a fraction of the grafts survive without intervention and some can be salvaged by urgent thrombectomy[4] and/or thrombolysis,[22] with revision of the arterial anastomosis. Unfortunately, retransplantation is restricted by a limited donor pool, especially in Japan, and even when the damaged liver is replaced, these patients often develop infectious and neurologic complications. Recently, however, there have been a few reports showing that, with early diagnosis, urgent reconstruction can reduce the need for retransplantation.[23,24]

With the introduction of color-Doppler ultrasound, a noninvasive, easy-to-perform, accurate, and portable diagnostic tool is available for the confirmation of vascular patency following liver transplantation. This allows for the liberal use of this modality in the postoperative care of the recipients. As most HAT occurs in the early period after liver transplantation, we believe

that examination by color-Doppler ultrasound on a daily basis is important to detect HAT before the graft suffers irreversible damage, as was emphasized by Nishida et al.[24] In our series, 8 of the 12 HAT patients did not experience hepatic failure.

In conclusion, female sex and metabolic disease are factors contributing to HAT after LDLT. More intensive anticoagulation therapy for this patient population might decrease the incidence of HAT and, thus, posttransplant recipient mortality.

References

1. Mori K, Nagata I, Yamagata S, Sasaki H, Nishizawa F, Takada Y, et al. The introduction of microvascular surgery to hepatic artery reconstruction in living donor liver transplantation: its surgical advantages compared with conventional procedures. Transplantation 1992;54:263–8.
2. Markmann JF, Markowitz JS, Yersiz H, Morrisey M, Farmer DG, Farmer DA, et al. Long-term survival after retransplantation of the liver. Ann Surg 1997;226:408–18.
3. Langnas AN, Marujo W, Stratta RJ, Wood RP, Li SJ, Shaw BW. Hepatic allograft rescue following arterial thrombosis: role of urgent revascularization. Transplantation 1991;51:86–90.
4. Klintmalm GB, Olson LM, Nery JR, Husberg BS, Paulsen AW. Treatment of hepatic artery thrombosis after liver transplantation with immediate vascular reconstruction: a report of three cases. Transplant Proc 1988;20:610–2.
5. Yanaga K, Lebeau G, Marsh JW, Gordon RD, Makowka L, Tzakis AG, et al. Hepatic artery reconstruction for hepatic artery thrombosis after orthotopic liver transplantation. Arch Surg 1990;125:628–31.
6. Pinna AD, Smith CV, Furukawa H, Starzl TE, Fung JJ. Urgent revascularization of liver allograft after early hepatic artery thrombosis. Transplantation 1996;62:1584–7.
7. Kawasaki S, Makuuchi M, Matsunami H, Hashikura Y, Ikegami T, Chisuwa H, et al. Preoperative measurement of segmental liver volume of donors for living-related liver transplantation. Hepatology 1993;18:1115–20.
8. Makuuchi M, Kawasaki S, Noguchi T, Hashikura Y, Matsunami H, Hayashi K, et al. Donor hepatectomy for living related partial liver transplantation. Surgery 1993;113:395–402.
9. Ikegami T, Kawasaki S, Matsunami H, Hashikura Y, Nakazawa Y, Miyagawa S, et al. Should all hepatic arterial branches be reconstructed in living-related liver transplantation? Surgery 1996;119:431–6.
10. Jain A, Reyes J, Kashyap R, Dodson SF, Demetris AJ, Ruppert K, et al. Long-term survival after liver transplantation in 4000 consecutive patients at a single center. Ann Surg 2000;232:490–500.
11. Yanaga K, Makowka L, Starzl TE. Is hepatic artery thrombosis after liver transplantation really a surgical complication? Transplant Proc 1989;21:3511–3.
12. Buckels JAC, Tisone G, Gunson BK, McMaster P. Low hematocrit reduces hepatic artery thrombosis after liver transplantation. Transplant Proc 1989;21:2460–1.
13. Langnas AN, Marujo W, Stratta RJ, Wood RP, Show BW. Vascular complication after orthotopic liver transplantation. Am J Surg 1991;161:76–83.
14. Mor E, Schwartz ME, Sheiner PA, Menesses P, Hytiroglou P, Emre S, et al. Prolonged preservation in University of Wisconsin solution associated with hepatic artery thrombosis safter orthotopic liver transplantation. Transplantation 1993;56: 1399–402.
15. Madalosso C, De Souza NF, Ilstrup DM, Wiesner RH, Krom RAF. Cytomegalovirus and its association with hepatic artery thrombosis after liver transplantation. Transplantation 1998;66: 294–7.
16. Gunsar F, Rolando N, Pastacaldi S, Patch D, Raimondo ML, Davidson B, et al. Late hepatic artery thrombosis after orthotopic liver transplantation. Liver Transpl 2003;9:605–11.
17. Samuel D, Gillet D, Castaing D, Reynes M, Bismuth H. Portal and arterial thrombosis in liver transplantation: a frequent even in severe rejection. Transplant Proc 1989;21:2225–7.
18. Oh CK, Pelletier SJ, Sawyer RG, Dacus AR, McCullough CS, Pruett TL, et al. Uni- and multivariate analysis of risk factors for early and late hepatic artery thrombosis after liver transplantation. Transplantation 2001;71:767–72.
19. Vivarelli M, Cucchetti A, La Barba G, Bellusci R, De Vivo A, Nardo B, et al. Ischemic arterial complications after liver transplantation in the adult: multivariate analysis of risk factors. Arch Surg 2004;139:1069–74.
20. Pastacaldi S, Teixeira R, Montalto P, Rolles K, Burroughs AK. Hepatic artery thrombosis after orthotopic liver transplantation: a review of nonsurgical causes. Liver Transpl 2001;7:75–81.
21. Drazan K, Shaked A, Olthoff KM, Imagawa D, Jurim O, Kiai K, et al. Etiology and management of symptomatic adult hepatic artery thrombosis after orthotopic liver transplantation (OLT). Am Surg 1996;62:237–40.
22. Figueras J, Busquets J, Dominguez J, Sancho C, Casanovas-Taltavull T, Rafecas A, et al. Intra-arterial thrombolysis in the treatment of acute hepatic artery thrombosis after liver transplantation. Transplantation 1995;59:1356–7.
23. Pinna AD, Smith CV, Furukawa H, Starzl TE, Fung JJ. Urgent revascularization of liver allografts after early hepatic artery thrombosis. Transplantation 1996;62:1584–7.
24. Nishida S, Kato T, Levi D, Naveen M, Thierry B, Vianna R, et al. Effect of protocol Doppler ultrasonography and urgent revascularization on early hepatic artery thrombosis after pediatric liver transplantation. Arch Surg 2002;137:1279–83.

Available online at www.sciencedirect.com
SCIENCE DIRECT®
ELSEVIER
Biochemical and Biophysical Research Communications 342 (2006) 434–440
BBRC
www.elsevier.com/locate/ybbrc

Development of liver regenerative therapy using glycoside-modified bone marrow cells

Ryosuke Misawa [a,c], Hirohiko Ise [a,*], Masafumi Takahashi [a], Hajime Morimoto [a], Eiji Kobayashi [b], Shin-ichi Miyagawa [c], Uichi Ikeda [a]

[a] *Department of Organ Regeneration, Institute of Organ Transplants, Reconstructive Medicine and Tissue Engineering, Shinshu University Graduate School of Medicine, 3-1-1 Asahi, Matsumoto, Nagano 390-8621, Japan*
[b] *Division of Organ Replacement Research, Center for Molecular Medicine, Jichi Medical School, 3311-1 Yakushiji, Minamikawachi, Tochigi 329-0431, Japan*
[c] *First Department of Surgery, Shinshu University School of Medicine, 3-1-1 Asahi, Matsumoto, Nagano 390-8621, Japan*

Received 5 January 2006
Available online 9 February 2006

Abstract

Several recent studies have reported that bone marrow cells (BMCs) have the ability to generate functional hepatocytes. However, the efficiency at which BMC transplantation generates functional hepatocytes is rather low. We assumed that if BMCs accumulated directly in liver, the functional BMC-derived hepatocytes should increase efficiently. We tried to increase the accumulation of BMCs directly in liver through the interaction between hepatic asialoglycoprotein receptor and desialylated BMCs. Desialylated BMCs were produced with treatment of neuraminidase. Desialylated BMCs that expressed green fluorescent protein (GFP) were injected into Long Evans Cinnamon (LEC) rats, a human Wilson's disease model, intravenously. At 3 and 5 months after transplantation, GFP-expressing hepatocyte nodules appeared in the liver of these BMC-transplanted LEC rats. These findings suggest that the functional BMC-derived hepatocytes can be generated by the direct accumulation of BMCs and that this strategy is new BMC therapy for liver regeneration.

Keywords: Bone marrow cells; Accumulation; Neuraminidase; Asialoglycoprotein receptor

Liver transplantation is one of the most important surgical means of saving the lives of patients suffering from otherwise fatal hepatic diseases, such as fulminant hepatitis and severe congenital liver failure. However, the therapy for these diseases is limited by a shortage of donors and by high costs. Hepatocyte transplantation may be considered as a potential alternative to whole-organ replacement in humans [1,2]. However, hepatocyte transplantation has not yet been established as a reliable alternative to liver transplantation, because it is difficult to obtain mature and intact hepatocytes.

Bone marrow transplantation has been effective in treating metabolic deficiencies, such as the fumarylacetoacetate hydrolase (FAH)-deficient mice with hereditary tyrosinemia type I [3]. However, it is known that the appearance of functional bone marrow cell (BMC)-derived hepatocytes remains a rare event after transplantation; in addition, in order to engraft another new BMCs in the liver and to allow for the appearance of functional BMC-derived hepatocytes, BMCs of a recipient must be replaced by another new BMCs by hematopoietic reconstitution with preparative lethal irradiation [4]. To realize the goal of implementing therapeutic BMC transplantation for liver disease as a reliable alternative to liver transplantation, the generation of functional BMC-derived hepatocytes must be raised efficiently in the host liver.

If the direct accumulation of BMCs in liver could increase without hematopoietic reconstitution in need of preparative lethal irradiation, the generation of functional

* Corresponding author. Fax: +81 263 37 2573.
E-mail address: ise@sch.md.shinshu-u.ac.jp (H. Ise).

0006-291X/$ - see front matter © 2006 Elsevier Inc. All rights reserved.
doi:10.1016/j.bbrc.2006.01.169

BMC-derived hepatocytes would increase efficiently and safely in the liver. To accumulate BMCs directly in the liver, we used asialoglycoprotein receptor (ASGPR) which exists on hepatocyte surface for receptor-mediated endocytosis and binds to galactose/*N*-acetylgalactosamine-terminated ligands [5,6]. We tried to accumulate BMCs directly in liver through specific interaction between desialylated BMCs and ASGPR. The desialylated BMCs were exposed to the galactose using neuraminidase (Nase) which removes the terminal sialic acid from glycoprotein located on the cell surface. We examined whether the treatment of BMCs with Nase resulted in enhanced engraftment of BMCs though ASGPR in the liver (Fig. 1A).

In this study, Long Evans Cinnamon (LEC) rats were used as the recipients for transplantation of desialylated BMCs. LEC rats constitute an authentic model for hepatic Wilson's disease (WD) [1,7,8]. WD is an autosomal-recessive disorder characterized by impaired biliary copper excretion, hypoceruloplasminemia, and copper toxicosis, due to mutations in the *atp7b* gene [9]. LEC rats develop acute hepatitis by progressive copper accumulation and are mortal around 4 months of age [1,7–9]. We hypothesized that if BMCs were accumulated in the damaged liver of the LEC rat, the appearance of BMC-derived hepatocyte is promoted and these hepatocytes compensate for loss of hepatic function in this liver. We treated green fluorescent protein (GFP)-expressing BMCs, which were isolated from GFP transgenic (Tg) rat, with Nase and transplanted these cells into LEC rats intravenously, and examined the appearance of BMC-derived hepatocytes by the expression of GFP and ATP7B.

Materials and methods

Animals. LEC rats were purchased from Charles River Japan, Inc. (Tokyo, Japan). Wistar and Tg rats (body weight: 180–250 g) were from Japan SLC, Inc. (Shizuoka, Japan). Albumin-Discosoma sp. Red fluorescent protein2 (Alb-DsRed2) Tg rats generated as described previously have liver-specific red fluorescent protein expression that is driven under the control of the albumin enhancer/promoter [10]. All experiments were approved by Shinshu University Guide for Laboratory Animals.

Nase treatment of bone marrow cells. BMCs were isolated from male Wistar, GFP Tg, and Alb-DsRed2 Tg rats. BMCs were flushed from the femoral and tibial bones of these rats and were prepared in Hanks' balanced salt solution (HBSS) (Invitrogen; Carlsbad, CA). These BMCs were then filtered through a 70-μm nylon mesh (Becton and Dickinson Company, Franklin Lakes, NJ). The BMCs (5×10^7 cells/mL) were incubated in HBSS containing 2 U/mL Nase type VI (5 U/mg protein; Sigma; St. Louis, MO) for 60 min at 4 °C. After Nase treatment, these cells were washed three times with Dulbecco's modified Eagle's medium (DMEM) (Sigma). Using trypan blue (Wako Pure Chemical Industries; Osaka,

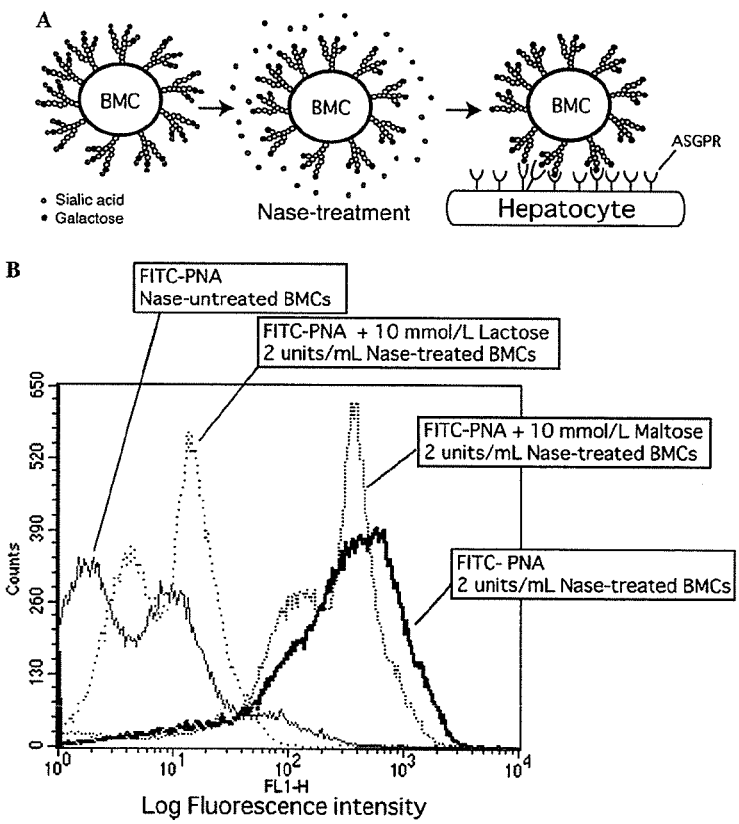

Fig. 1. Procedure and flow cytometric analysis for desialylated BMCs. (A) Procedure to expose galactose on BMC surface by Nase-treatment. (B) Flow cytometric analysis for 2 U/mL Nase-treated and -untreated BMCs using FITC-conjugated PNA staining. Solid bold line, FITC-PNA-stained Nase-treated BMCs; shaded area, FITC-PNA-stained Nase-untreated BMCs; smooth dotted line, PNA-FITC-stained Nase-treated BMCs with 10 mmol/L maltose; rough dotted line, FITC-PNA-stained Nase-treated BMCs with 10 mmol/L lactose.

Japan) exclusion, we confirmed that no damaged BMCs were caused by Nase treatment. Nase treatment has been reported with no effect on hematopoietic activity of BMCs [11,12].

Cell staining and flow cytometric analysis. The Nase-treated and -untreated BMCs were incubated in HBSS containing 5 μg/mL fluorescein isocyanate-conjugated peanut agglutinin (FITC-PNA) (Seikagaku Corporation; Tokyo, Japan) for 30 min at 4 °C. Flow cytometric analysis was carried out using FACS Calibur (Becton Dickinson and Company).

Hepatocyte preparation. Rat primary hepatocytes were isolated from the livers of male rats using a modified in situ perfusion method [2,13]. Briefly, dead parenchymal hepatocytes were completely removed by density gradient centrifugation using Percoll (Amersham Bioscience; Buckinghamshire, UK). The viable parenchymal hepatocytes were then suspended in DMEM containing antibiotics (50 μg/mL penicillin, 50 μg/mL streptomycin, and 100 μg/mL neomycin) (Invitrogen). Hepatocytes with ⩾99% viability were used in this study.

Interaction of Nase-treated BMCs and hepatocytes. Nase-treated and -untreated BMCs were labeled using the PKH26 red fluorescent cell linker kit (Sigma). The Nase-treated or -untreated PKH26-labeled BMCs (3×10^5cells) were cocultured with hepatocytes (3×10^5 cells) in DMEM containing 10% fetal bovine serum (FBS; Biowest; Rue de la Caille, France) at 37 °C. At 0.5, 1, and 24 h after these BMCs were seeded onto the monolayer, the medium was replaced by fresh medium and the unattached BMCs were removed. The BMCs bound to hepatocytes were observed using fluorescence microscopy (IX-70, Olympus Corporation; Tokyo, Japan), and the number of these bound BMCs on randomly 10 independent areas was measured by NIH Image software (Bethesda, MD).

To examine the accumulation of these BMCs into normal liver in vivo, these BMCs were labeled by 5 μg/mL Calcein AM (Wako Pure Chemical Industries) and Calcein AM-labeled BMCs (1×10^7 cells) were intravenously injected into rat. At 3 and 24 h after injection, cryosections (10-μm thick) were prepared from these BMC-transplanted livers and immediately observed by fluorescent microscopy. The number of accumulated BMCs in the liver was counted on randomly 10 sections from these rats ($n = 3$, each time point).

Detection of DsRed2- and GFP-expressing hepatocytes in coculture. We isolated BMCs from Alb-DsRed2 Tg rat and cocultured these cells with hepatocytes from GFP Tg rat [10]. The Nase-treated or -untreated BMCs (3×10^5 cells) from Alb-DsRed2 Tg rat were incubated on a GFP-expressing hepatocyte monolayer (3×10^5 cells). The cocultured cells were incubated in DMEM containing 1 mg/mL insulin, 50 ng/mL epidermal growth factor, and 10% FBS. At 5 days of incubation, the cells were fixed in 4% paraformaldehyde (PFA) (Nacalai Tesque; Kyoto, Japan) for 30 min at 4 °C and were incubated overnight at 4 °C with rabbit anti-DsRed2 IgG (BD Biosciences Clontech; Palo Alto, CA) as the primary antibody. DsRed2-expressing hepatocytes were detected by rabbit anti-DsRed2 IgG antibody, because we could not distinguish between DsRed2-expressing hepatocytes and normal hepatocytes, due to strong red auto-fluorescence of hepatocyte. After the cells were washed with phosphate-buffered saline (PBS), they were incubated with peroxidase-conjugated anti-rabbit IgG (Zymed Laboratories; South San Francisco, CA). Peroxidase enzyme activity was detected with 3,3-diaminobenzidine (Vector; Burlingame, CA) as the substrate. The GFP-expressing hepatocytes were detected by fluorescence microscopy.

Transplantation of BMCs from GFP Tg rat into LEC rat. Nase-treated and -untreated BMCs (5×10^7 cells) from GFP Tg rat were injected into 16-week-old LEC rats 4 times over a period of 4 weeks or 10 times over 10 weeks, once per week, intravenously. Cyclosporin A (Wako Pure Chemical Industries) was administered with 10 mg/kg/day as an immunosuppressant for the full treatment period. Rats were sacrificed and livers were examined to observe and to analyze the transplanted BMCs. Each animal group received transplants of both types of BMCs ($n = 3$, each).

Detection of BMC-derived hepatocytes. The transplanted BMC-derived cells in the host livers were detected by observing GFP fluorescence. For the observation of GFP fluorescence and immunohistochemical staining for albumin and ASGPR, cryosections (10-μm thick) from the host livers were fixed in 4% PFA for 15 min before being incubated overnight at 4 °C with rabbit anti-rat albumin IgG (Cappel; Cochranville, PA) and rabbit anti-rat ASGPR-1 antiserum [2] as the primary antibodies, respectively. This rabbit anti-mouse ASGPR-1 antiserum has been previously made by our laboratory and recognizes the extracellular domain of mouse and rat ASGPR-1 [2]. After the sections were washed with PBS, they were incubated with Cy3-conjugated anti-rabbit IgG (Seikagaku Corporation) as the secondary antibodies.

Laser capture microdissection, the extraction of total RNA, and reverse transcription-polymerase chain reaction. To investigate gene expression in the GFP-expressing nodules, we used laser capture microdissection (LCM) and reverse transcription-polymerase chain reaction (RT-PCR). The LCM for GFP-expressing nodules and extraction of total RNA from these nodules were performed by Takara Biochemicals (Tokyo, Japan). The total RNA was extracted from two GFP-expressing nodules (about 2000 cells per nodule), normal liver sections of LEC rat (GFP-negative cells), and whole livers by Isogen (Wako Pure Chemical Industries). Single-stranded complementary DNA was synthesized from 2 ng or 2 μg total RNA using the SuperScript III™ First-strand Synthesis System for RT-PCR (Invitrogen). The PCR was performed using the *Taq* PCR kit (Qiagen; Hilden, Germany), according to previously published technique [1]. Briefly, the PCR for rat atp7b, β-actin, and albumin gene was performed using the atp7b primers (sense 5′-CCATCTCCAGTGACATCAG-3′; anti-sense 5′-AGTCCCAATAGCAATGCC-3′), β-actin primers (sense 5′-GGAGAAGATTTGGCACCAC-3′; anti-sense 5′-AGGCATACAGGGACAACAC-3′; nonamplified intron sequence, nucleotide positions 1694–2157), and rat albumin primers (sense 5′-TCCATTCACACTCTCTTCGG-3′; anti-sense 5′-AATTCTGCAAGCACTGTGCC-3′). PCR for atp7b, β-actin, and rat albumin included denaturing at 94 °C for 1 min, annealing at 60 °C for 1 min, and extension at 72 °C for 2 min.

Measurement of oxidative activity of serum ceruloplasmin. The oxidase activity of ceruloplasmin was measured by incubating 10 μL serum with 20 μg 3,3′-dimethoxybenzidine dihydrochloride (1 mg/mL *o*-dianisidine; Sigma) in a final volume of 100 μL of 0.1 mol/L sodium acetate, pH 5.6, for 5 and 15 min at 37 °C [14]. The reaction was stopped by adding 100 μL concentrated sulfuric acid. Absorbance was read at 540 nm with respective serum blanks containing sodium azide to inhibit oxidase activity. Normal rat serum served as a standard. The oxidative activity of ceruloplasmin = $(\text{Absorbance}_{15\,\text{min}} - \text{Absorbance}_{5\,\text{min}}) \times 6.25 \times 10^2$ U/L.

Statistical analysis. A one-tailed unpaired Student's *t* test was used to generate *P* values and determine the significance of all quantified differences in number of the adhesion of BMCs to hepatocyte monolayer and liver between Nase-treated and -untreated BMCs. Data were expressed as mean values ± SD using $P < 0.05$ as the criterion of significance.

Results and discussion

Expression of terminal galactose residues on surfaces of BMCs by Nase treatment

To examine whether Nase treatment enhanced the expression of the terminal galactose residues on the BMC surface, we performed flow cytometric analysis of the Nase-treated BMCs using FITC-PNA staining. The normal BMCs were stained slightly. BMCs that are expressing terminal galactose residues on surface might innately exist in the population of bone marrow cells, without Nase treatment (Fig. 1B). However, the Nase-treated BMCs were stained more intensely than normal BMCs (Nase-untreated). In addition, the staining of FITC-PNA to the Nase-treated BMCs was inhibited by 10 mmol/L lactose but not by 10 mmol/L maltose (Fig. 1B). These results showed that Nase treatment resulted in the striking expression of terminal galactose residues on the BMC surface.

Enhanced interaction through ASGPR between Nase-treated BMCs and hepatocytes

We examined whether Nase-treated BMCs could recognize hepatocytes through the interaction between ASGPR of the hepatocytes and terminal galactose residues on surface of Nase-treated BMCs. When Nase-treated and -untreated BMCs were allowed to bind to a hepatocyte monolayer, the binding of Nase-treated BMCs was augmented in vitro, compared with that of Nase-untreated BMCs (Fig. 2A). These results indicate that ASGPR on the cell surface facilitates the binding of Nase-treated BMCs to hepatocytes. Next, to examine whether Nase-treated BMCs would accumulate into normal liver in vivo, these BMCs were intravenously injected into rat. We found that the Nase-treated BMCs accumulated in the liver more than the Nase-untreated BMCs (Fig. 2B).

To investigate whether BMCs that were cocultured with hepatocytes could acquire the characteristics of hepatocyte, we used Alb-DsRed2 Tg rats that have a liver-specific reporter gene expression of red fluorescent protein [10] and cocultured BMCs from these rats with hepatocytes from the GFP Tg rats. At 5 days of coculture, we detected DsRed2-expressing hepatocytes and the number of DsRed2-expressing hepatocytes was 9.1 ± 1.9 or 4.5 ± 1.5 cells/cm^2 in coculture of Nase-treated or -untreated Alb-DsRed2 BMCs with GFP-expressing hepatocytes, respectively. We found that all DsRed2-expressing hepatocytes expressed GFP simultaneously (Fig. 3).

These results suggest that DsRed2-expressing cells are derived from BMC and acquire the characteristics of hepatocytes, and moreover, the Nase treatment promotes the appearance of BMC-derived hepatocytes in vitro by at least in part cell fusion.

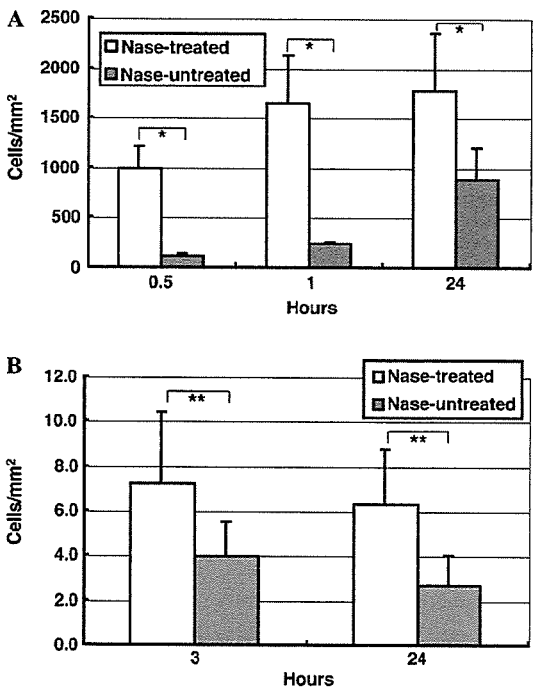

Fig. 2. Interaction between Nase-treated or -untreated BMCs and hepatocyte monolayer and accumulation of Nase-treated or -untreated BMCs in liver. (A) Number of Nase-treated or -untreated BMCs adhering to hepatocyte monolayer at 0.5, 1, and 24 h after BMC seeding to the monolayer. Each column represents the group mean ± SD of 10 independent areas. $^*P < 0.05$. (B) Number of Nase-treated or -untreated BMCs accumulating into liver at 3 and 24 h after BMC injection. Each column represents the group mean ± SD of 30 independent areas in 3 rats for each time point. $^{**}P < 0.01$. White bar, Nase-treated BMCs; black bar, Nase-untreated BMCs.

Generation of BMC-derived hepatocytes in LEC rat liver by transplantation of Nase-treated BMCs

To investigate whether BMC-derived hepatocytes increased in liver, we transplanted 5×10^7 cells of Nase-treated or -untreated BMCs into LEC rats once per week for 4 or 10 weeks intravenously. To distinguish between transplanted BMCs and recipient hepatocytes, transplanted BMCs were isolated from GFP Tg rats. Table 1 shows the number and size of GFP-expressing nodules in Nase-treated and -untreated BMC-transplanted LEC rats. The total number of GFP-expressing nodules in liver of Nase-treated BMC-transplanted LEC rats was more than that of Nase-untreated BMC-transplanted LEC rats at 3 months after transplantation. In both the Nase-treated and -untreated groups, the GFP-expressing nodules had diameters of about 200 μm at 3 months after

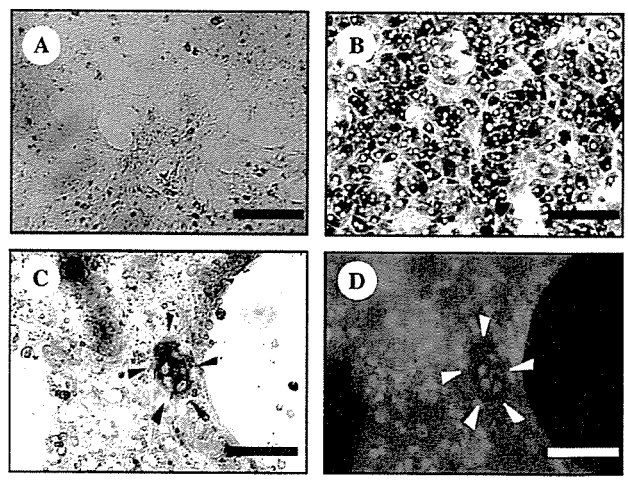

Fig. 3. DsRed2 immunocytochemical analysis in coculture of Nase-treated Alb-DsRed2 Tg BMCs with GFP-expressing hepatocyte monolayer at 5 days after BMC seeding to the monolayer. (A) Normal hepatocyte monolayer (negative control). (B) DsRed2-expressing hepatocytes isolated from Alb-DsRed2 Tg rat (positive control; immunostaining by anti-DsRed2 antibody). Scale bars indicate 200 μm. (C,D) Coculture of Nase-treated Alb-Red2 Tg BMCs with GFP-expressing hepatocyte monolayer. DsRed2-expressing hepatocytes are indicated by black arrowheads (C) and GFP fluorescence image of GFP-expressing hepatocyte monolayer (D) and white arrowheads indicated DsRed2-expressing hepatocytes. Scale bars indicate 100 μm. (For interpretation of the references to color in this figure legend, the reader is referred to the web version of this paper.)

Table 1
Summary of Nase-treated or -untreated BMCs-transplanted LEC rats

Transplanted BMCs	Survival	Sacrificed months (frequency of transplantation)	GFP-expressing nodules (30 sections)	Size of nodule (μm)
Nase-treated				
1	S	3 (4)	39	~200
2	S	3 (4)	15	~200
3	S	3 (4)	20	~200
4	S	5 (4)	36	500–1000
5	D	— (4)	—	—
6	D	— (4)	—	—
Nase-untreated				
1	S	2 (4) (died in 2 months)	10	~200
2	S	3 (4)	6	~200
3	D	— (4)	—	—
4	D	— (4)	—	—
5	D	— (4)	—	—
6	D	— (4)	—	—

S, survivor by sacrifice; D, death by sacrifice.

transplantation. The GFP-expressing nodules in LEC rats that the Nase-treated BMC were transplanted into reached diameters of approximately 500–1000 μm at 5 months after transplantation (Table 1). To examine the ability of these GFP-expressing nodules to have the hepatic functions, the expression of albumin and ASGPR in these nodules was examined by immunohistochemical staining. The GFP-expressing nodules demonstrated the expression of albumin and ASGPR (Fig. 4).

To investigate whether the GFP-expressing nodules expressed ATP7B, we performed LCM in these nodules, extracted total RNA from dissected nodules, and examined the mRNA expression levels of ATP7B, albumin, and β-actin in these nodules by RT-PCR. The GFP-expressing cells expressed ATP7B and albumin (Fig. 5A). The GFP-expressing nodules in the whole liver were too few to detect the expression of ATP7B at 3 and 5 months after fourth transplantation of BMCs. However, the expression of ATP7B in the whole liver was clearly detected at 5 months after 10th transplantation of the Nase-treated BMCs (Fig. 5B). The activity of ceruloplasmin was also approximately 21%–24% of the normal rat level in the Nase-treated BMC-transplanted LEC rats at 5 months after the 10th transplantation (LEC rats: 11.0 U/L, Nase-treated GFP-BMC-transplanted LEC rats: 40.0 U/L, and normal rats: 168.0 U/L), and the GFP-expressing nodules in these rats occupied approximately 2.4% of total liver mass from the calculation of a number and size of these nodules.

The frequency of GFP-expressing hepatocytes increased in the group with transplantation of Nase-treated GFP-BMCs, compared with that of Nase-untreated GFP-BMCs. These hepatocytes had not only normal hepatic function but also *atp7b*, the lacking gene in the LEC rat. These results suggest that the directly accumulating BMCs in liver could promote the appearance of BMC-derived hepatocytes.

It is curious to investigate whether BMC-derived hepatocytes were generated by cell fusion or transdifferentiation.

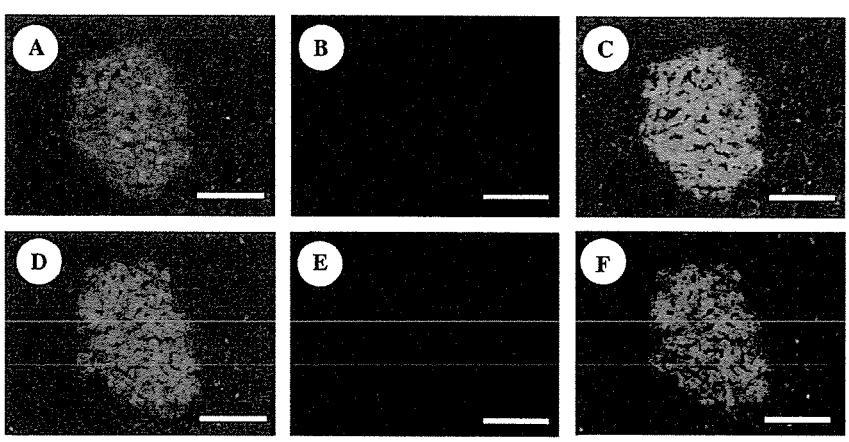

Fig. 4. Immunohistochemical analysis of albumin and ASGPR for GFP-expressing nodules in liver of LEC rat at 3 months after the fourth transplantation of Nase-treated GFP-BMCs. GFP fluorescence image (A), immunohistochemical image of albumin (B), and merged image of GFP fluorescence and albumin immuno-staining (C). GFP fluorescence image (D), immunohistochemical image of ASGPR (E), and merged image of GFP fluorescence and ASGPR immuno-staining (F). Scale bars indicate 100 μm.

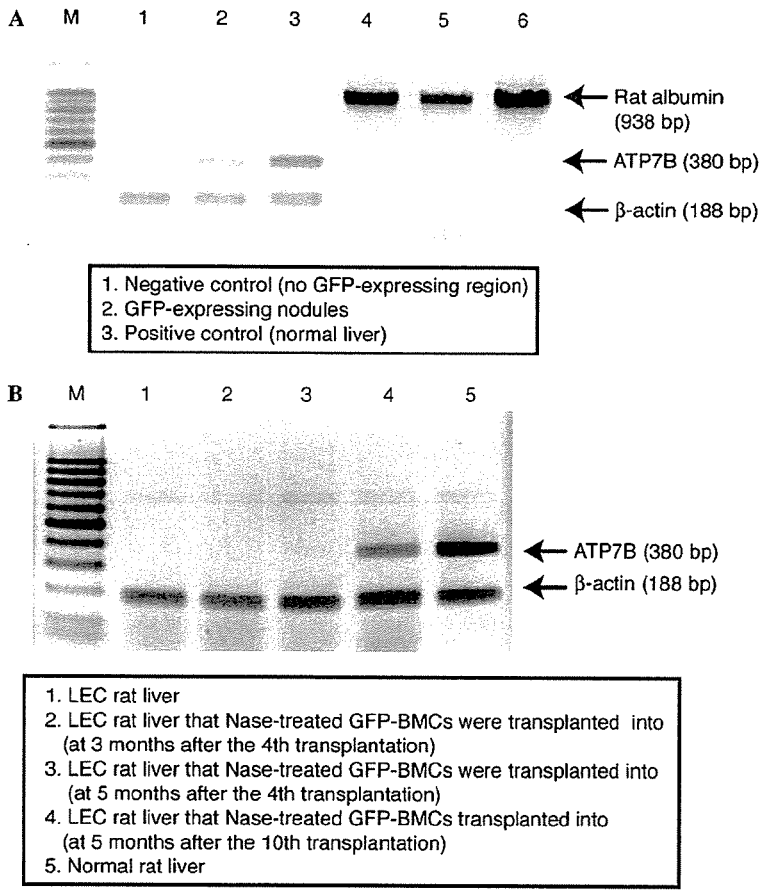

Fig. 5. Expression of ATP7B in liver of LEC rats with transplanted Nase-treated GFP-BMCs. (A) Expression of ATP7B and albumin in GFP-expressing nodules dissected by LCM. RT-PCR analysis of the dissected no GFP-expressing region (lane 1,4), GFP-expressing nodules (lane 2,5), and ATP7B-expressing region in normal liver (lane 3,6). (B) ATP7B expression in whole liver of LEC rat with transplanted Nase-treated GFP-BMCs. Whole liver of LEC rat (negative control) (lane 1), whole liver of LEC rat transplanted with Nase-treated GFP-BMCs at 3 months (lane 2), 5 months (lane 3) after the fourth transplantation, 5 months after the 10th transplantation (lane 4), and whole liver of normal rat (positive control) (lane 5). M, 100 bp DNA ladder marker.

Since there are numbers of reports that BMC-derived hepatocytes are generated by both fusion and transdifferentiation [3,4,10,15–20], we focused on the development of strategy for accumulation of BMCs in the liver in this study. However, in vitro experiments, we demonstrated that BMC-derived hepatocytes might be mainly generated by cell fusion. Further investigation was required to elucidate the precise mechanism of BMC-derived hepatocytes in vivo.

It is important to find BMC fractions that are facilitated to fuse or transdifferentiate into hepatocytes in order to achieve more efficient therapeutic system by transplantation of a small number of BMCs. Myelomonocytic cells such as macrophages are reported to fuse to hepatocytes [16,17]. Therefore, if Nase-treated myelomonocytic cells are transplanted into LEC rats, the appearance of many BMC-derived nodules may be realized more efficiently by the transplantation of a small number of cells.

Concluding remarks

In conclusion, we have demonstrated that direct accumulation of desialylated BMCs into liver increased the proportion of functional BMC-derived hepatocytes that transferred new BMC-derived genes such as ATP7B and GFP, and complemented the deleted function in LEC rats. This strategy would enable us to provide an aid for development of safer BMC therapy for liver regeneration without hematopoietic reconstitution in need of preparative irradiation.

Acknowledgments

We are grateful to Junko Yano, Tomoko Hamaji, and Kazuko Misawa for excellent technical assistance. This work was supported in part by a Grant-in-Aid for Scientific Research from the Ministry of Education, Science, Sports, and Culture of Japan.

References

[1] H. Malhi, A.N. Irani, I. Volenberg, M.L. Schilsky, S. Gupta, Early cell transplantation in LEC rats modeling Wilson's disease eliminates hepatic copper with reversal of liver disease, Gastroenterology 122 (2002) 438–447.

[2] H. Ise, T. Nikaido, N. Negishi, N. Sugihara, F. Suzuki, T. Akaike, U. Ikeda, Effective hepatocyte transplantation using rat hepatocytes with low asialoglycoprotein receptor expression, Am. J. Pathol. 165 (2004) 501–510.
[3] E. Lagasse, H. Connors, M. Al-Dhalimy, M. Reitsma, M. Dohse, L. Osborne, X. Wang, M. Finegold, I.L. Weissman, M. Grompe, Purified hematopoietic stem cells can differentiate into hepatocytes in vivo, Nat. Med. 6 (2000) 1229–1234.
[4] X. Wang, E. Montini, M. Al-Dhalimy, E. Lagasse, M. Finegold, M. Grompe, Kinetics of liver repopulation after bone marrow transplantation, Am. J. Pathol. 161 (2002) 565–574.
[5] R.J. Stocket, The asialoglycoprotein receptor: relationships between structure, function, and expression, Physiol. Rev. 75 (1995) 591–609.
[6] L. Dini, L. Conti-Devirgiliis, S. Russo-Caia, The galactose-specific receptor system in rat liver during development, Development 100 (1987) 13–22.
[7] Y. Li, Y. Togashi, S. Sato, T. Emoto, J.H. Kang, N. Takeichi, H. Kobayashi, Y. Kojima, Y. Une, J. Uchino, Spontaneous hepatic copper accumulation in Long-Evans Cinnamon rats with hereditary hepatitis. A model of Wilson's disease, J. Clin. Invest. 87 (1991) 1858–1861.
[8] A.N. Irani, H. Malhi, S. Slehria, G.R. Gorla, I. Volenberg, M.L. Schilsky, S. Gupta, Correction of liver disease following transplantation of normal rat hepatocytes into Long-Evans Cinnamon rats modeling Wilson's disease, Mol. Ther. 3 (2001) 302–309.
[9] K. Terada, T. Sugiyama, The Long-Evans Cinnamon rat: an animal model for Wilson's disease, Pediatr. Int. 41 (1999) 414–418.
[10] Y. Sato, Y. Igarashi, Y. Hakamata, T. Murakami, T. Kaneko, M. Takahashi, N. Seo, E. Kobayashi, Establishment of Alb-DsRed2 transgenic rat for liver regeneration research, Biochem. Biophys. Res. Commun. 311 (2003) 478–481.
[11] T. Nagahama, K. Sugiura, S. Lee, H. Morita, Y. Adachi, A.H. Kwon, Y. Kamiyama, S. Ikehara, A new method for tolerance induction: busulfan administration followed by intravenous injection of neuraminidase-treated donor bone marrow, Stem Cells 19 (2001) 425–435.
[12] T. Suda, S. Sano, S. Hori, T. Azuma, N. Tateishi, T. Hamaoka, H. Fujiwara, Prevention of suppression of alloreactive capacity following intravenous injection of neuraminidase-treated allogeneic cells by co-injection of agents competing for asialoglycoprotein receptor, Reg. Immunol. 1 (1988) 24–31.
[13] H. Ise, N. Sugihara, N. Negishi, T. Nikaido, T. Akaike, Low asialoglycoprotein receptor expression as markers for highly proliferative potential hepatocytes, Biochem. Biophys. Res. Commun. 285 (2001) 172–182.
[14] K.H. Schosinsky, H.P. Lehmann, M.F. Beeler, Measurement of ceruloplasmin from its oxidase activity in serum by use of *o*-dianisidine dihydrochloride, Clin. Chem. 20 (1974) 1556–1563.
[15] Y.Y. Jang, M.I. Collector, S.B. Baylin, A.M. Diehl, S.J. Sharkis, Hematopoietic stem cells convert into liver cells within days without fusion, Nat. cell biol. 6 (2004) 532–539.
[16] H. Willenbring, A.S. Bailey, M. Foster, Y. Akkari, C. Dorrell, S. Olson, M. Finegold, W.H. Fleming, M. Grompe, Myelomonocytic cells are sufficient for therapeutic cell fusion in liver, Nat. Med. 10 (2004) 744–748.
[17] F.D. Camargo, M. Finegold, M.A. Goodell, Hematopoietic myelomonocytic cells are the major source of hepatocyte fusion partners, J. Clin. Invest. 113 (2004) 1266–1270.
[18] G. Vassilopoulos, P.R. Wang, D.W. Russell, Transplanted bone marrow regenerates liver by cell fusion, Nature 422 (2003) 901–904.
[19] S. Terai, I. Sakaida, N. Yamamoto, K. Omori, T. Watanabe, S. Ohata, T. Katada, K. Miyamoto, K. Shinoda, H. Nishina, K. Okita, An in vivo model for monitoring trans-differentiation of bone marrow cells into functional hepatocytes, J. Biochem. (Tokyo) 134 (2003) 551–558.
[20] B.E. Petersen, W.C. Bowen, K.D. Patrene, W.M. Mars, A.K. Sullivan, N. Murase, S.S. Boggs, J.S. Greenberger, J.P. Goff, Bone marrow as a potential source of hepatic oval cells, Science 284 (1999) 1168–1170.